

Dry and Wet Lab Studies for Some Indole Derivatives as Possible Corrosion Inhibitors for Copper in 2M HNO₃

Hala.M.Hassan^{1*}, Awad Al-Rashdi², A.Attia³ and A.M.Eldesoky⁴

^{1*}Textile Technology Department, Industrial Education College, Beni-Suef University, Egypt and Chemistry Department, Faculty of Science, Jazan University, KSA. E-mail: dr.halamahfooz@yahoo.com

²Al-Qunfudah Center for Scientific Research (QCSR), Chemistry Department, Al-Qunfudah University College, Umm Al-Qura University, KSA.

³Department of Chemistry ,Faculty of Science, Mansoura University, Mansoura ,Egypt and Faculty of Science and Arts in Balgarn , Chemistry Department, King Khalid University, KSA.

⁴Engineering Chemistry Department, High Institute of Engineering & Technology (New Damietta), Egypt and Al-Qunfudah Center for Scientific Research (QCSR), Al-Qunfudah University College, Umm Al-Qura University ,KSA.

Abstract—With contrast to the traditional techniques of identifying new corrosion inhibitors in wet lab, a prior dry-lab process, followed by a wet-lab process is suggested by using cheminformatics tools. Quantum chemical method is used to explore the relationship between the inhibitor molecular properties and its inhibition efficiency. The density function theory (DFT) is also used to study the structural properties of two selected indole derivatives in aqueous phase. It is found that when the indole derivatives adsorb on the copper surface, molecular structure influences their interaction mechanism. The inhibition efficiencies of these compounds showed a certain relationship to highest occupied molecular orbital (HOMO) energy, Mulliken atomic charges and Fukui indices. A wet lab study has been carried out using weight loss, potentiodynamic polarization, electrochemical impedance spectroscopy (EIS) and Electrochemical frequency modulation (EFM) measurements to evaluate their inhibition performance in 2 M HNO₃ solutions at 30° C. Adsorption takes place by a direct chemisorption on the exposed copper surface, while it most probably occurs via hydrogen bonding on the oxidized surface. Compound (1) was the most effective among the two tested inhibitors, while Compound (2) was less effective than Compound (1). Results obtained from dry-lab process are in good agreement with those recorded from wet-lab experiments.

Keywords: Wet-lab Experiments, Indole Derivatives, Copper, HNO₃, EFM, EIS.

1 INTRODUCTION

Copper (Cu) metallisation has been used in integrated circuits for high-speed logic devices instead of the conventional aluminium (Al)-alloy metallisation because of its excellent electrical and thermal conductivity [1-3]. However, it is well known that Cu is very susceptible to corrosion in aqueous media and the corrosion products cause a decrease in the electrical conductivity of the devices [4,5]. Thus, much attention has been focused on the behaviour of various inhibitors in different media to find the conditions for preventing Cu corrosion. Many investigators [6-9] have studied to obtain optimum corrosion protection for Cu in various aqueous solutions by either finding new inhibitors or improving the inhibition efficiency [10]. Most acid corrosion inhibitors are nitrogen (N), sulfur, or oxygen containing organic compounds. Among these compounds it is generally known that heterocyclic compounds, especially N-based ones, are effective inhibitors for Cu corrosion in aqueous solutions [11]. Especially, imidazole and its derivatives are of interest as corrosion inhibitors for Cu metals and alloys [12-15]. Imidazole is a planar, aromatic heterocyclic organic compound with two N atoms forming part of a five membered ring [16]. One of the N atoms is of the pyrrole type and the other is a pyridine-like one. Despite extensive studies undertaken on imidazole, until now, it is still questionable what mechanism is adequate for the explanation of the inhibition of Cu corrosion by imidazole in acid solutions.

The objective of this work is to identify two selected indole derivatives in dry-lab process as possible corrosion inhibitors for copper in 2M HNO₃. Highest occupied molecular orbital (E_{HOMO}), lowest unoccupied molecular orbital (E_{LUMO}), dipole moment, charges on atoms and total energy was analyzed through an evaluation of the Fukui indices. These parameters have been calculated using DFT (density function theory) methods. From the results obtained in the dry lab, we could identify the studied molecules as possible corrosion inhibitors for copper in 2M HNO₃ in our laboratory, which investigated experimentally by weight loss, potentiodynamic polarization, electrochemical impedance spectroscopy (EIS) and Electrochemical frequency modulation (EFM) measurements. The surface morphology of inhibited copper was analyzed by scanning electron microscope technology with energy dispersive X-ray spectroscopy ((SEM-EDX).

2 Experimental Details

2.1 Composition of Material Samples

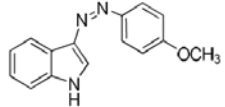
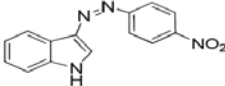
TABLE 1
CHEMICAL COMPOSITION OF THE COPPER IN WEIGHT %

Element	Sn	Ag	Fe	Zn	Pb	As	Cu
Weight %	0.001	0.001	0.01	0.05	0.002	0.0002	The rest

2.2 Chemicals and Solutions

Nitric acid (BDH grade) and organic additives, The organic inhibitors used in this study were some organic compounds [17], listed in Table (2)

TABLE 2
CHEMICAL STRUCTURE, NAMES, MOLECULAR WEIGHTS AND MOLECULAR FORMULA OF INHIBITORS

Compound No.	Structure	Name	Mol. Wt. / M. Formula
(1)		(Z)-3-((4-methoxyphenyl) diazenyl)-1H-indole	251.28 C ₁₅ H ₁₅ N ₃ O
(2)		(Z)-3-((4-nitrophenyl) diazenyl)-1H-indole	266.25 C ₁₅ H ₁₃ N ₃ O ₂

2.3 Methods Used for Corrosion Measurements

2.3.1 Weight Loss Tests

For weight loss measurements, square specimens of size 2cm x 2cm x 0.2cm were used. The specimens were first polished to a mirror finish using 400 and 800 grit emery paper, immersed in methanol and finally washed with bidistilled water and dried before being weighed and immersed into the test solution. The weight loss measurements were carried out in a 100ml capacity glass beaker placed in water thermostat. The specimens were then immediately immersed in the test solution without or with desired concentration of the investigated compounds. Triplicate specimens were exposed for each condition and the mean weight losses were reported in order to verify reproducibility of the experiments.

2.3.2 Potentiodynamic Polarization Measurements

Polarization experiments were carried out in a conventional three-electrode cell with platinum gauze as the auxiliary electrode (1 cm²) and a saturated calomel electrode (SCE) coupled to a fine Luggin capillary as reference electrode. The working electrode was in the form of a square cut from copper sheet of equal composition embedded in epoxy resin of polytetrafluoroethylene so that the flat surface area was 1 cm². Prior to each measurement, the electrode surface was pretreated in the same manner as the weight loss experiments. Before measurements, the electrode was immersed in solution at natural potential for 30 min. until a steady state was reached. The potential was started from - 600 to + 400 mV vs. open circuit potential (E_{ocp}). All experiments were carried out in freshly

prepared solutions at 25°C and results were always repeated at least three times to check the reproducibility.

2.3.3 Electrochemical Impedance Spectroscopy Measurements

Impedance measurements were carried out using AC signals of 5mV peak to peak amplitude at the open circuit potential in the frequency range of 100 kHz to 0.1Hz. All impedance data were fitted to appropriate equivalent circuit using the Gamry Echem Analyst software.

2.3.4 Electrochemical Frequency Modulation Technique

EFM experiments were performed with applying potential perturbation signal with amplitude 10mV with two sine waves of 2 and 5 Hz. The choice for the frequencies of 2 and 5 Hz was based on three arguments [18]. The larger peaks were used to calculate the corrosion current density (i_{corr}), the Tafel slopes (β_c and β_a) and the causality factors CF-2 and CF-3 [19].

All electrochemical experiments were carried out using Gamry instrument PCI300/4 Potentiostat/Galvanostat/Zra analyzer, DC105 corrosion software, EIS300 electrochemical impedance spectroscopy software, EFM140 electrochemical frequency modulation software and Echem Analyst 5.5 for results plotting, graphing, data fitting and calculating.

2.3.5 SEM-EDX Measurement

The copper surface was prepared by keeping the specimens for 3 days in 2M HNO₃ in the presence and absence of optimum concentration of investigated organic derivatives, after abraded using different emery papers up to 1200 grit size and then polished with Al₂O₃ (0.5m particles size), after this immersion time, the specimens were washed gently with bidistilled water, carefully dried and mounted into the spectrometer without any further treatment. The corroded copper surfaces were examined using an X-ray diffractometer Philips (pw-1390) with Cu-tube (Cu K_{α1}, λ = 1.54051 Å), a scanning electron microscope (SEM, JOEL, JSM-T20, Japan).

2.3.6 Theoretical Study

Accelrys (Material Studio Version 4.4) software for quantum chemical calculations has been used.

3 Results and Discussion

3.1 Weight Loss Measurements

Fig. (1): represents the weight loss-time curves in the absence and presence of different concentrations of compound (1). Similar curves were obtained for other inhibitors (not shown). Table (3) collects the values inhibition efficiency obtained from weight loss measurements in 2M HNO₃ at 30 ± 0.1 °C. The results of this Table show that the presence of inhibitors reduce the corrosion rate of copper in 2M HNO₃ and hence, increase the inhibition efficiency. The inhibition achieved by these compounds decreases in the following order: Compound (1) > Compound (2).

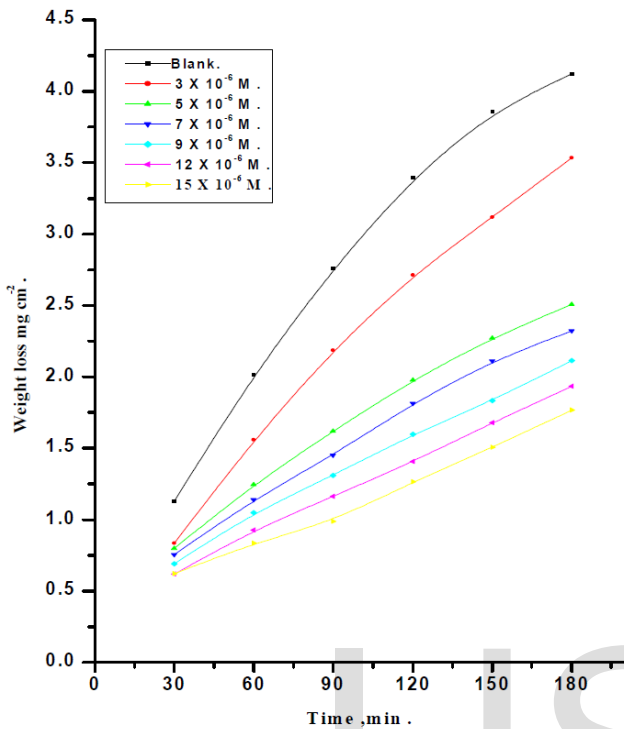


Fig. 1: Weight-Loss Time Curves for the Dissolution of Copper in the Absence and Presence of Different Concentrations of Compound (1) at 30 ± 0.1 °C.

TABLE 3

VARIATION OF INHIBITION EFFICIENCY (%IE) OF DIFFERENT COPOUNDS WITH THEIR MOLAR CONCENTRATIONS AT 30 ± 0.1°C FROM WEIGHT LOSS MEASUREMENTS AT 90 MIN IMMERSION IN 2M HNO₃.

COMPOUND	CONC., M	% IE
BLANK	---	---
(1)	3X10 ⁻⁶	21.2
	5X10 ⁻⁶	26.8
	7X10 ⁻⁶	41.8
	9X10 ⁻⁶	47.8
	12X10 ⁻⁶	53.0
	15X10 ⁻⁶	68.0
(2)	3X10 ⁻⁶	11.2
	5X10 ⁻⁶	25.3
	7X10 ⁻⁶	34.5
	9X10 ⁻⁶	41.7
	12X10 ⁻⁶	51.3
	15X10 ⁻⁶	64.8

3.2 Adsorption Isotherm

It is widely acknowledge that adsorption isotherm provide useful insight onto the mechanism of corrosion inhibition

as well as the interaction among the adsorbed molecules themselves and their interaction with the electrode surface [20]. In this study, Temkin adsorption isotherm was found to be suitable for the experimental results. The isotherm is described by the following equation:

$$\theta = 2.303/a \log K_{ads} + 2.303/a \log C \quad (1)$$

Where C is the inhibitor concentration, K_{ads} is the adsorption equilibrium constant. The plot of θ versus log C was linear relation (shown in Figure 2). And the adsorption equilibrium constant K_{ads} can be calculated from the intercept. Also ΔG^o_{ads} can be calculated from the following equation:

$$\log K_{ads} = -\log 55.5 - \Delta G^o_{ads} / 2.303RT \quad (2)$$

Where value of 55.5 is the concentration of water in solution in mole/liter [21], R is the universal gas constant and T is the absolute temperature. It was appear that the value of ΔG^o_{ads} has a negative sign ensure the spontaneity of the adsorption and stability of the adsorbed layer on the alloy surface [22]. Also the values of ΔG^o_{ads} around 40 kJ mol⁻¹ which was attributed to electrostatic interactions between inhibitors species and the charged metal surface (physisorption). The values of K_{ads} were found to run parallel to the % IE [K (1) > K (2)]. This result reflects the increasing capability, due to structural formation, on the metal surface [23].

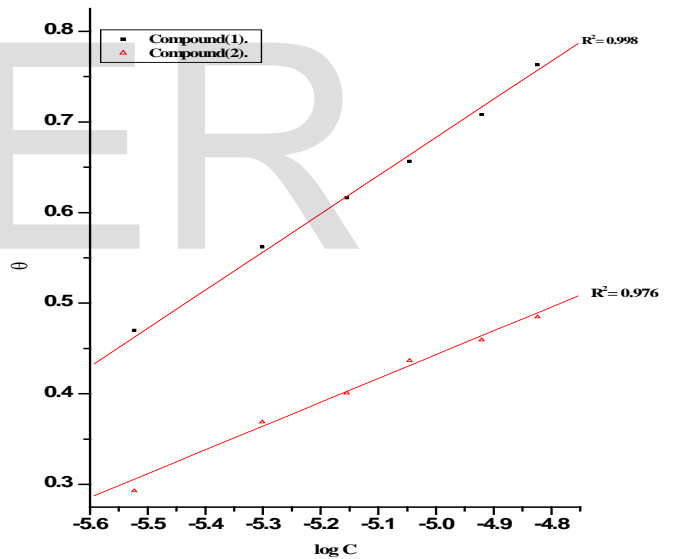


Fig. 2: Curve Fitting of Corrosion Data for Copper in 2M HNO₃ in Presence of Different Concentrations of Inhibitors Corresponding to Temkin Adsorption Isotherm at 30 ± 0.1 °C.

TABLE 4

INHIBITOR BINDING CONSTANT (K), FREE ENERGY OF BINDING (ΔG_{ADS.}), AND LATER INTERACTION PARAMETER (A) FOR INHIBITORS AT 30 ± 0.1 °C.

INHIBITORS	TEMKIN		
	A	K	-ΔG _{ADS.} , kJmol ⁻¹
Compound (1)	10.2	1.45	11.2

Compound (2)	6.1	1.18	9.4
--------------	-----	------	-----

3.3 Effect of Temperature

The effect of temperature on the inhibited acid-metal reaction is highly complex, because many changes occur on the metal surface, such as rapid etching and desorption of the inhibitor and the inhibitor itself, in some cases, may undergo decomposition and/or rearrangement. Generally the corrosion rate increases with the rise of temperature. It was found that the inhibition efficiency decreases with increasing temperature and increases with increasing the concentration of the inhibitor. The activation energy (E_a^*) of the corrosion process was calculated using Arrhenius equation [24]:

$$C.R. = A \exp(-E_a^* / RT) \quad (3)$$

Where C.R. corrosion rate, A is Arrhenius constant, R is the gas constant and T is the absolute temperature. The values of activation energies E_a^* can be obtained from the slope of the straight lines of plotting log C.R. vs. $1/T$ in the presence and absence of investigated compounds at various temperatures Figure (3) and are given in Table (5), it is noted that the values of activation energy increase in the presence of inhibitors and with increase of the concentration of the inhibitors. This is due to the presence of a film of inhibitors on copper surface. The activation energy for the corrosion of copper in 2 M HNO_3 was found to be 33.1 kJ mol^{-1} which is in good agreement with the work carried out by Fouda et al [25] and others [26-27] An alternative formulation of the Arrhenius equation is the transition state equation 4 [28]:

$$C.R. = RT/Nh \exp(\Delta S^*/R) \exp(-\Delta H^*/RT) \quad (4)$$

Where h is Planck's constant, N is Avogadro's number, ΔS^* is the entropy of activation and ΔH^* is the enthalpy of activation. Figure (4) shows a plot of $\log(C.R. / T)$ vs. $(1/T)$. Straight lines are obtained with a slope of $(\Delta H^*/2.303 R)$ and an intercept of $(\log R/Nh + \Delta S^*/2.303 R)$ from which the values of ΔH^* and ΔS^* are calculated and also listed in Table (5). From inspection of Table (5) it is clear that the positive values of ΔH^* reflect that the process of adsorption of the inhibitors on the copper surface is an endothermic process; it is attributable unequivocally to chemisorption [29]. Typically, the enthalpy of a chemisorption process approaches 100 kJ mol^{-1} . More interesting behavior was observed in Table (5) that positive ΔS^* values is accompanied with endothermic adsorption process. This is agrees with what expected, when the adsorption is an endothermic process, it must be accompanied by an increase in the entropy energy change and vice versa [30].

It is seen that investigated derivatives have inhibiting properties at all the studied temperatures and the values of % IE decrease with temperature increase. This shows that the inhibitor has experienced a significant decrease in its protective properties with increase in temperature. This decrease in the protective properties of the inhibitor with increase in temperature may be connected with two effects; a certain drawing of the adsorption-desorption equilibrium towards desorption (meaning that the

strength of adsorption process decreases at higher temperatures) and roughening of the metal surface which results from enhanced corrosion. These results suggest that physical adsorption may be the type of adsorption of the inhibitor on the copper surface.

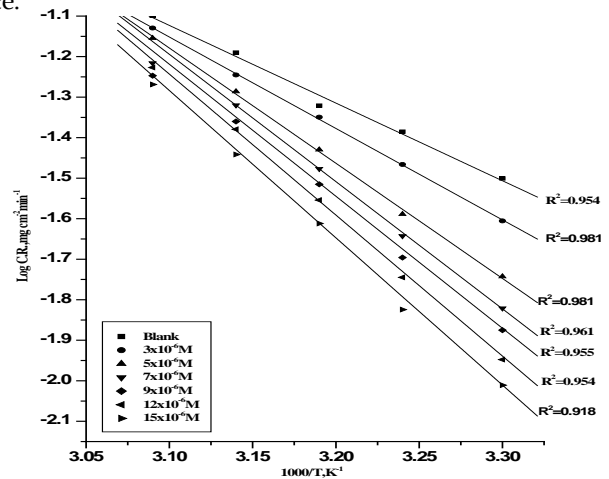


Fig. 3: Arrhenius (Plots) for Corrosion of Copper in 2M HNO_3 in the Absence and Presence of Different Concentrations of Compound (1)

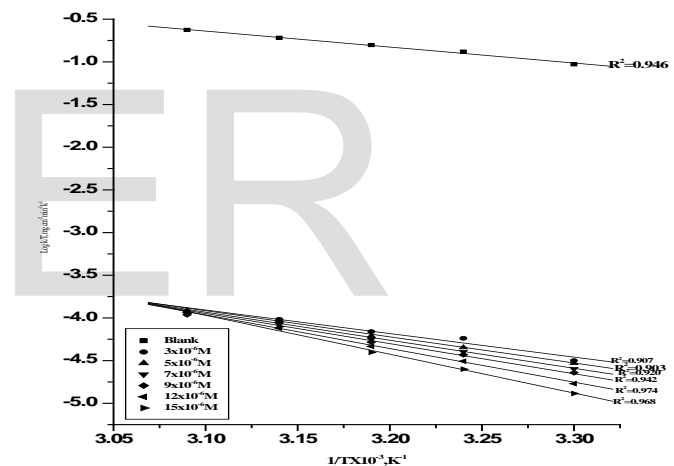


Fig. 4: Plots of $(\log k/T)$ vs. $1/T$ for the Corrosion of Copper in 2M HNO_3 in the Absence and Presence of Different Concentrations of Compound (1)

TABLE 5

ACTIVATION PARAMETERS FOR THE DISSOLUTION OF COPPER IN THE PRESENCE AND ABSENCE OF DIFFERENT CONCENTRATIONS OF INHIBITORS IN 2M HNO_3

Compound	Conc., M	E_a^* kJ mol^{-1}	ΔH^* kJ mol^{-1}	$-\Delta S^*$ $\text{J mol}^{-1} \text{K}^{-1}$
Blank	0.0	33.1	33.5	119.9
(1)	3×10^{-6}	55.3	55.7	52.3
	5×10^{-6}	61.2	61.4	34.5
	7×10^{-6}	66.3	65.5	21.2
	9×10^{-6}	69.0	69.4	16.9
	12×10^{-6}	79.2	77.1	16.3
	15×10^{-6}	89.4	89.1	15.2
(2)	3×10^{-6}	42.9	42.4	91.3
	5×10^{-6}	56.3	57.0	47.3
	7×10^{-6}	61.9	60.5	44.6
	9×10^{-6}	63.7	62.9	28.9

3.4 Potentiodynamic Polarization Measurements

Theoretically, copper can hardly be corroded in the deoxygenated acid solutions, as copper cannot displace hydrogen from acid solutions according to the theories of chemical thermodynamics [31-33]. However, this situation will change in nitric acid. Dissolved oxygen may be reduced on copper surface and this will allow corrosion to occur. It is a good approximation to ignore the hydrogen evolution reaction and only consider oxygen reduction in the nitric acid solutions at potentials near the corrosion potentials [34].

Polarization measurements were carried out in order to gain knowledge concerning the kinetics of the cathodic and anodic reactions. Figure (5): shows the polarization behavior of copper electrode in 2 M HNO₃ in the absence and presence of various concentrations of compound (1). Figure (5) shows that both the anodic and cathodic reactions are affected by the addition of investigated organic derivatives and the inhibition efficiency increases as the inhibitor concentration increases, but the cathodic reaction is more inhibited, meaning that the addition of organic derivatives reduces the anodic dissolution of copper and also retards the cathodic reactions. Therefore, investigated organic derivatives are considered as mixed type inhibitors.

The values of electrochemical parameters such as corrosion current densities (*i*_{corr}), corrosion potential (*E*_{corr}), the cathodic Tafel slope (β_c), anodic Tafel slope (β_a) and inhibition efficiency (% IE) were calculated from the curves of Figure (5) and are listed in Table (6). The results in Table (6) revealed that the corrosion current density decreases obviously after the addition of inhibitors in 2 M HNO₃ and % IE increases with increasing the inhibitor concentration. In the presence of inhibitors *E*_{corr} was enhanced with no definite trend, indicating that these compounds act as mixed-type inhibitors in 2M HNO₃. The inhibition efficiency was calculated using equation 5:

$$\%IE = \frac{(i_{ocorr} - i_{corr})}{i_{ocorr}} \times 100 \quad (5)$$

Where *i*_{ocorr} and *i*_{corr} are the uninhibited and inhibited corrosion current densities, respectively.

Also it is obvious from Table (6) that the slopes of the anodic (β_a) and cathodic (β_c) Tafel lines remain almost unchanged upon addition of organic derivatives, giving rise to a nearly parallel set of anodic lines, and almost parallel cathodic plots results too. Thus the adsorbed inhibitors act by simple blocking of the active sites for both anodic and cathodic processes. In other words, the adsorbed inhibitors decrease the surface area for corrosion without affecting the corrosion mechanism of copper in 2 M HNO₃ solution, and only causes inactivation of a part of the surface with respect to the corrosive medium [35,36]. The inhibition efficiency of these compounds follows the sequence: compound (1) > compound (2).

This sequence may attribute to free electron pair in oxygen atom, π electrons on aromatic nuclei and the substituent in the molecular structure of the inhibitor, and again reflects, as confirmed from weight loss measurements, the increased ability of compound (1) to inhibit nitric acid corrosion of copper as compared to compound (2). This is clearly seen from the highest efficiency recorded for compound (1).

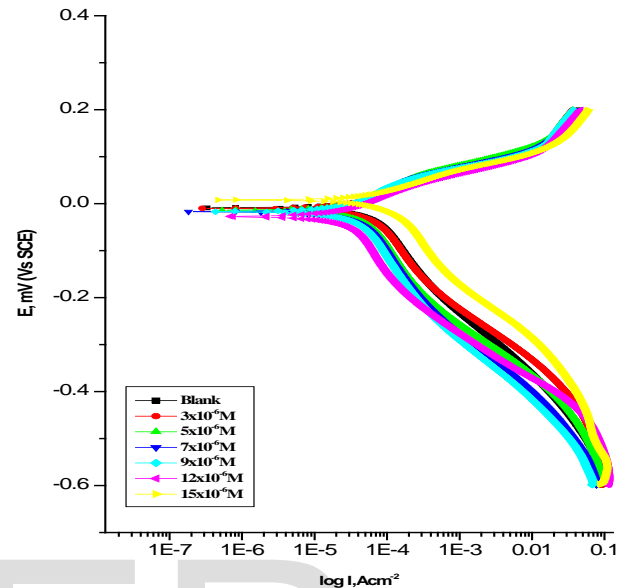


Fig. 5: Potentiodynamic Polarization Curves for the Corrosion of Copper in 2M HNO₃ in the Absence and Presence of Various Concentrations of Compound (1) at 30 ± 0.1 °C

TABLE 6

EFFECT OF CONCENTRATIONS OF THE INVESTIGATED COMPOUNDS ON THE FREE CORROSION POTENTIAL (*E*_{CORR}), CORROSION CURRENT DENSITY (*I*_{CORR}), TAFEL SLOPES (β_a & β_c), DEGREE OF SURFACE COVERAGE (θ) AND INHIBITION EFFICIENCY (% IE) FOR COPPER IN 2M HNO₃ AT 30 ± 0.1 °C.

Compound	Conc. M.	- <i>E</i> _{corr} , mV, vs. SCE	<i>i</i> _{corr} μA cm ²	β_c mV dec ⁻¹	β_a mV dec ⁻¹	θ	% IE
(1)	0.0	784	183.2	198	77	---	---
	3X10 ⁻⁶	677	48.5	171	69	0.735	73.5
	5X10 ⁻⁶	536	43.5	190	64	0.762	76.2
	7X10 ⁻⁶	264	34.5	181	84	0.811	81.1
	9X10 ⁻⁶	211	30.4	187	69	0.834	83.4
	12X10 ⁻⁶	276	19.3	185	69	0.894	89.4
	15X10 ⁻⁶	232	18.1	125	49	0.901	90.1
(2)	3X10 ⁻⁶	743	73.6	273	92	0.598	59.8
	5X10 ⁻⁶	612	61.7	230	74	0.663	66.3
	7X10 ⁻⁶	523	51.9	218	91	0.716	71.6
	9X10 ⁻⁶	488	48.0	277	91	0.737	73.7
	12X10 ⁻⁶	398	34.5	217	87	0.811	81.1
	15X10 ⁻⁶	299	27.9	186	67	0.847	84.7

3.5 Electrochemical Impedance Spectroscopy (EIS)

EIS is well-established and powerful technique in the study of corrosion. Surface properties, electrode kinetics and mechanis-

tic information can be obtained from impedance diagrams [37-41]. Figure (6) shows the Nyquist (a) and Bode (b) plots obtained at open-circuit potential both in the absence and presence of increasing concentrations of investigated compounds at 30 ± 0.1 °C. The increase in the size of the capacitive loop with the addition of organic derivatives shows that a barrier gradually forms on the copper surface. The increase in the capacitive loop size (Figure 6a) enhances, at a fixed inhibitor concentration, following the order: compound (1) > compound (2), confirming the highest inhibitive influence of compound (1). Bode plots (Figure 6b), shows that the total impedance increases with increasing inhibitor concentration ($\log Z$ vs. $\log f$). But ($\log f$ vs. phase), also Bode plot shows the continuous increase in the phase angle shift, obviously correlating with the increase of inhibitor adsorbed on copper surface. The Nyquist plots do not yield perfect semicircles as expected from the theory of EIS. The deviation from ideal semicircle was generally attributed to the frequency dispersion [42] as well as to the inhomogeneities of the surface. EIS spectra of the organic additives were analyzed using the equivalent circuit, Figure (7), which represents a single charge transfer reaction and fits well with our experimental results. The constant phase element, CPE, is introduced in the circuit instead of a pure double layer capacitor to give a more accurate fit [43]. The double layer capacitance, C_{dl} , for a circuit including a

$$C_{dl} = Y_0 \omega n^{-1} / \sin [n (\pi/2)] \quad (6)$$

where Y_0 is the magnitude of the CPE, $\omega = 2\pi f_{max}$, f_{max} is the frequency at which the imaginary component of the impedance is maximal and the factor n is an adjustable parameter that usually lies between 0.50 and 1.0. After analyzing the shape of the Nyquist plots, it is concluded that the curves approximated by a single capacitive semicircles, showing that the corrosion process was mainly charged-transfer controlled [45, 46]. The general shape of the curves is very similar for all samples (in presence or absence of inhibitors at different immersion times) indicating that no change in the corrosion mechanism [47]. From the impedance data (Table 7), we conclude that the value of R_{ct} increases with increasing the concentration of the inhibitors and this indicates an increase in % IE, which in concord with the weight loss results obtained.

In fact the presence of inhibitors enhances the value of R_{ct} in acidic solution. Values of double layer capacitance are also brought down to the maximum extent in the presence of inhibitor and the decrease in the values of CPE follows the order similar to that obtained for i_{corr} in this study. The decrease in CPE/C_{dl} results from a decrease in local dielectric constant and/or an increase in the thickness of the double layer, suggesting that organic derivatives inhibit the iron corrosion by adsorption at metal/acid [48, 49]. The inhibition efficiency was calculated from the charge transfer resistance data from equation 7 [50]:

$$\% IE_{EIS} = [1 - (R_{ct}^0 / R_{ct})] \times 100 \quad (7)$$

Where R_{ct}^0 and R_{ct} are the charge-transfer resistance values without and with inhibitor respectively.

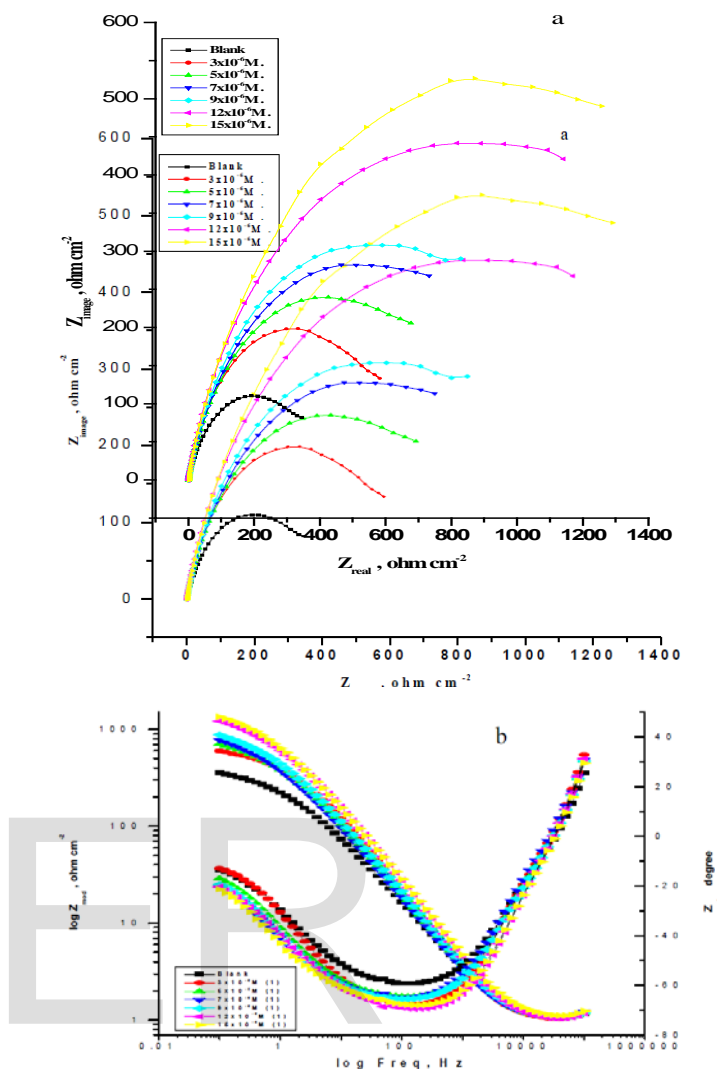


Fig. 6: The Nyquist (a) and Bode (b) Plots for Corrosion of Copper in 2M HNO_3 in Absence and Presence of Different Concentrations of Compound (1) at 30 ± 0.1 °C

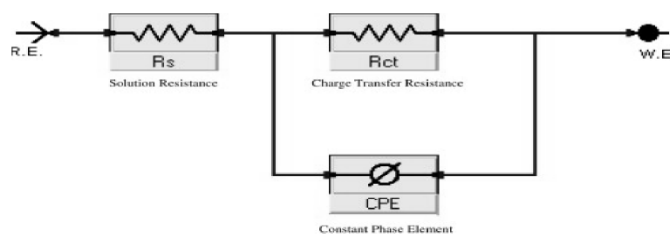


Fig. 7: Equivalent Circuit Model Used to Fit Experimental EIS

TABLE 7

ELECTROCHEMICAL KINETIC PARAMETERS OBTAINED BY EIS TECHNIQUE FOR COPPER IN 2M HNO₃ WITHOUT AND WITH VARIOUS CONCENTRATIONS OF TWO COMPOUNDS AT 30 °C.

Compound	Conc. M	R _s × 10 ³ Ω cm ²	Y × 10 ⁶	n × 10 ³	R _r Ω cm ²	C _{dl} μF cm ²	θ	% IE
Blank	0.0	991.0	542.9	738.8	297.7	327.7	-----	-----
(1)	3X10 ⁻⁶	972.0	358.0	786.8	553.8	231.2	0.462	46.2
	5X10 ⁻⁶	904.5	332.3	805.6	556.7	225.0	0.465	47.0
	7X10 ⁻⁶	984.4	315.6	781.9	570.1	212.1	0.477	52.6
	9X10 ⁻⁶	997.7	247.0	785.5	681.5	207.0	0.563	56.3
	12X10 ⁻⁶	974.8	210.3	824.9	780.1	153.0	0.618	61.8
	15X10 ⁻⁶	976.0	186.6	818.0	965.6	123.0	0.691	69.1
(2)	3X10 ⁻⁶	970.0	369.0	804.5	364.8	226.0	0.183	18.3
	5X10 ⁻⁶	900.1	336.3	789.8	561.7	224.0	0.470	46.7
	7X10 ⁻⁶	900.2	327.8	805.0	629.0	219.0	0.526	47.6
	9X10 ⁻⁶	902.0	315.3	795.1	677.3	211.0	0.560	56.0
	12X10 ⁻⁶	995.3	301.2	806.4	697.5	202.0	0.573	57.3
	15X10 ⁻⁶	911.2	287.3	793.0	891.8	192.0	0.666	66.6

3.6 Electrochemical Frequency Modulation Technique (EFM)

EFM is a nondestructive corrosion measurement technique that can directly and quickly determine the corrosion current values without prior knowledge of Tafel slopes, and with only a small polarizing signal. These advantages of EFM technique make it an ideal candidate for online corrosion monitoring [51]. The great strength of the EFM is the causality factors which serve as an internal check on the validity of EFM measurement. The causality factors CF-2 and CF-3 are calculated from the frequency spectrum of the current responses.

Figure (8) shows the EFM Intermodulation spectrums of copper in nitric acid solution containing different concentrations of compound (1). Similar curves were obtained for other compounds (not shown). The harmonic and intermodulation peaks are clearly visible and are much larger than the background noise. The two large peaks, with amplitude of about 200 μA, are the response to the 40 and 100 mHz (2 and 5 Hz) excitation frequencies. It is important to note that between the peaks there is nearly no current response (<100 nA). The experimental EFM data were treated using two different models: complete diffusion control of the cathodic reaction and the "activation" model. For the latter, a set of three non-linear equations had been solved, assuming that the corrosion potential does not change due to the polarization of the working electrode [52]. The larger peaks were used to calculate the corrosion current density (i_{corr}), the Tafel slopes (β_c and β_a) and the causality factors (CF-2 and CF-3). These electrochemical parameters were listed in Table (8). The data presented in Table (8) obviously show that, the addition of any one of tested compounds at a given concentration to the acidic solution decreases the corrosion current density, indicating that these compounds inhibit the corrosion of copper in 2 M HNO₃ through adsorption. The causality factors obtained under dif-

ferent experimental conditions are approximately equal to the theoretical values (2 and 3) indicating that the measured data are verified and of good quality. The inhibition efficiencies % I_{EFM} increase by increasing the inhibitor concentrations and was calculated as from equation 8:

$$\%I_{EFM} = [1 - (i_{corr} / i_{ocorr})] \times 100 \quad (8)$$

Where i_{ocorr} and i_{corr} are corrosion current densities in the absence and presence of inhibitor, respectively.

The inhibition sufficiency obtained from this method is in the order: compound (1) > compound (2).

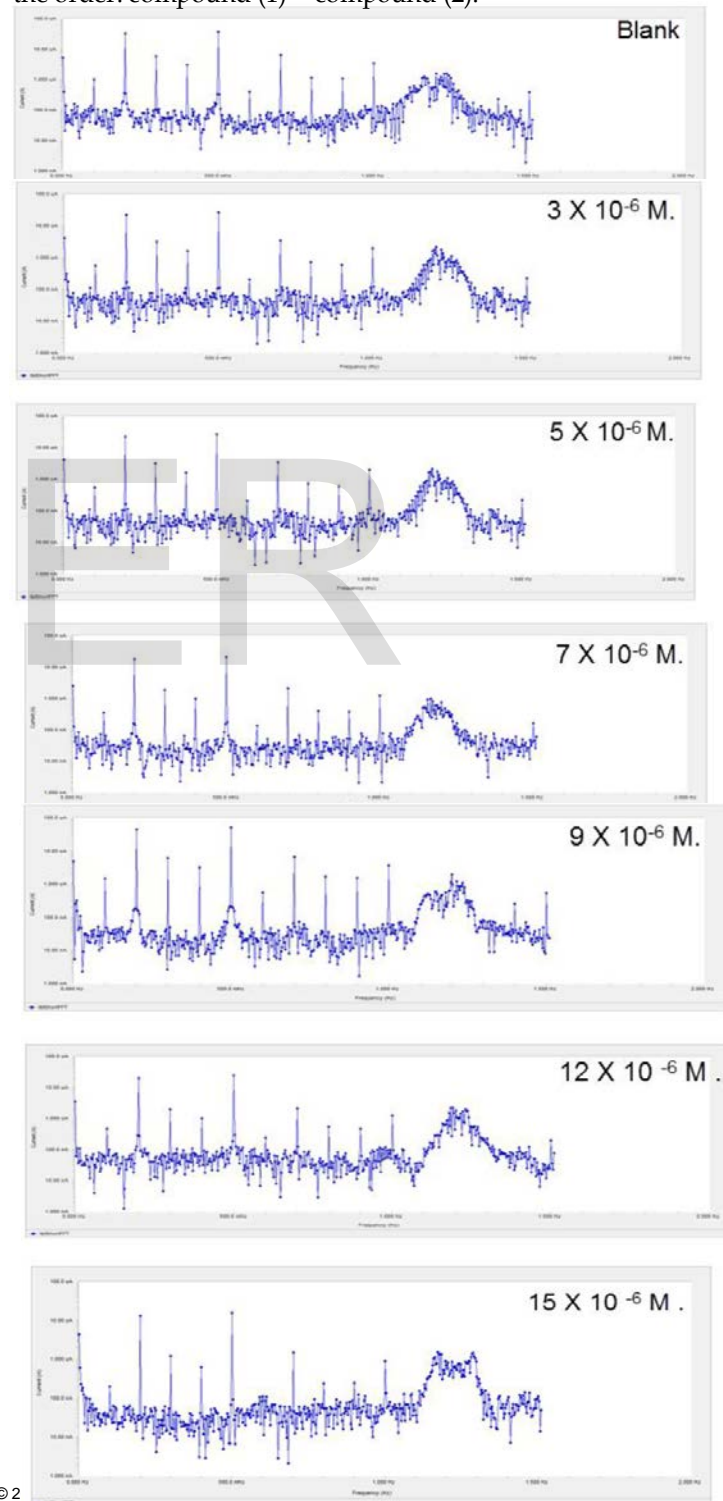


Fig. 8: EFM Spectra for Copper in 2M HNO₃ in the Absence and Presence of Different Concentrations of Compound (1)

TABLE 8
 ELECTROCHEMICAL KINETIC PARAMETERS OBTAINED BY EFM
 TECHNIQUE FOR COPPER IN 2M HNO₃ WITHOUT AND WITH VARIOUS
 CONCENTRATIONS OF TWO COMPOUNDS AT 30°C.

Compound	Conc., M.	i_{cor} , $\mu A\ cm^{-2}$	β_c , $mV\ dec^{-1}$	β_a , $mV\ dec^{-1}$	CF-2	CF-3	θ	% IE
Blank	0.0	50.20	96	53	1.90	3.07	-----	-----
(1)	3X10 ⁻⁶	24.92	104	68	1.69	2.09	0.503	50.3
	5X10 ⁻⁶	23.93	99	58	2.03	3.12	0.523	52.3
	7X10 ⁻⁶	21.77	118	78	1.73	2.81	0.566	56.6
	9X10 ⁻⁶	21.09	76	53	1.84	3.68	0.579	57.9
	12X10 ⁻⁶	17.97	104	56	1.75	3.11	0.642	64.2
	15X10 ⁻⁶	13.24	71	57	1.72	3.19	0.736	73.6
(2)	3X10 ⁻⁶	40.80	126	54	1.85	2.99	0.187	18.7
	5X10 ⁻⁶	24.46	91	52	1.89	3.23	0.512	51.2
	7X10 ⁻⁶	24.02	108	65	1.78	3.13	0.521	52.1
	9X10 ⁻⁶	21.71	119	67	1.84	2.23	0.567	56.7
	12X10 ⁻⁶	20.47	129	74	1.79	2.41	0.592	59.2
	15X10 ⁻⁶	18.26	104	66	2.01	3.67	0.636	63.6

3.7 SEM Investigation and EDX Analysis

The formation of a protective surface film of inhibitor at the electrode surface was further confirmed by SEM observations of the metal surface. Also, in order to see whether the organic derivatives molecules are adsorbed on the copper surface or not, both SEM and EDX experiments were carried out. Figure (9) shows the Scanning Electron Microscopy (SEM) micrograph of fresh copper surface without any additions of acid or the inhibitor. The morphological images for copper surface exposed to 2 M HNO₃ solution without and with the addition of the optimum concentration of the organic derivatives are shown in Figure (9). As can be seen, there was a marked improvement in the surface morphology of copper that was treated with the inhibitor (the rate of corrosion is suppressed) due to the formation of an adsorbed protective film of the inhibitor at the sample surface.

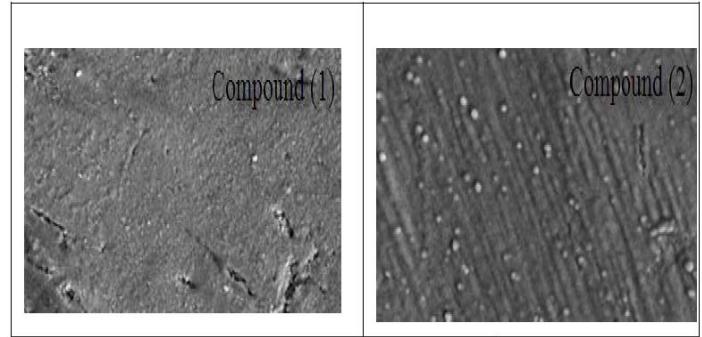
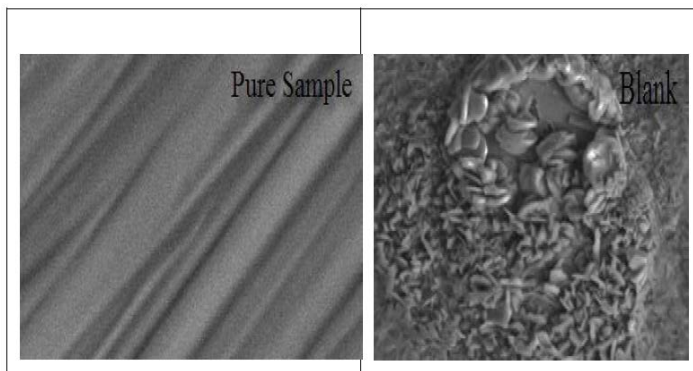


Fig. 9: SEM Micrographs for Copper in Absence and Presence of 15x10⁻⁶ M of Organic Compounds

The corresponding Energy dispersive X-ray (EDX) profile analysis is presented in Figure (10). The EDX survey spectra were used to determine which elements of inhibitor were present on the electrode surface before and after exposure to the inhibitor solution. For the specimen without inhibitor treatment [Figure 10] only copper was detected. This is confirmed by using XRD, the main corrosion products formed on exposed copper to nitric acid were identified as the basic copper nitrate, gerhardtite (Cu₂(NO₃)(OH)₃) and to a smaller extent cuprite (Cu₂O) [53, 54]. It is noticed the existence of the carbon, oxygen and nitrogen peak in the EDX spectra in the case of the sample exposed to the inhibitor, could be attributed to the adsorption of organic moiety at the copper surface. The increase in amount of carbon atom in the case of compound (1) (13.19 %) in comparison of compounds (2) (12.17%), indicated that the dissolution of copper is very inhibited by compound (1) and thereby shows a very high protective capacity, in contrast, the protective films formed by the compound (2) is very thin, especially in the case of compound (2). Also a strong enrichment with carbon is noted in the case of compound (1) (Table 9). The spectra of Figure (10) show that the oxygen signals are considerably suppressed relative to the samples prepared in 2M HNO₃ solution, and certainly this suppression will increase with increasing investigated concentrations and immersion time. The suppression of the oxygen signals takes place because of the overlying inhibitor film. Also it is important to notice the amount of copper peaks of EDX spectra is increased in the presence of inhibitor in a comparison of EDX analysis obtained in the absence of inhibitor may indicating that the investigated derivatives molecules protecting the copper surface against acid corrosion, in addition to the surface of the metal may not covered completely by the investigated molecules due to the short immersion time. The composition of the detected elements on the copper surface indicates that the inhibitor molecules are strongly adsorbed on the copper forming a Cu- investigated molecule bond, thus preventing the surface against corrosion.



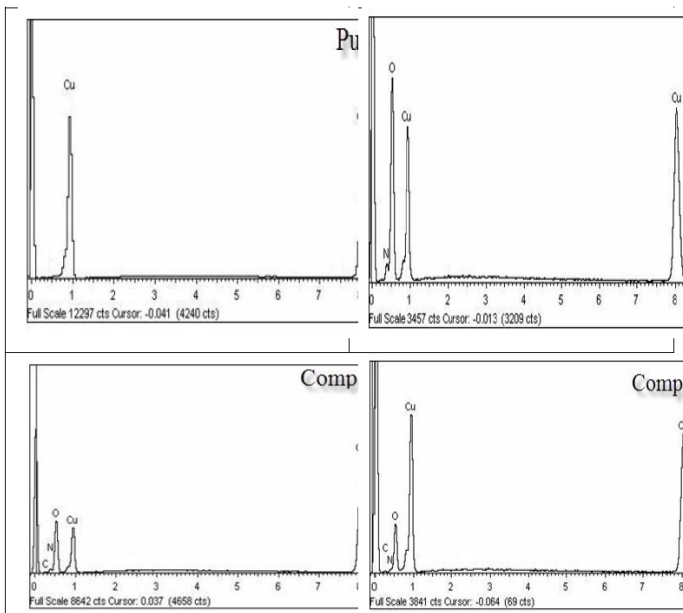


Fig. 10: EDX Analysis for Copper in Absence and Presence of $15 \times 10^{-6} \text{M}$ for 3 Days Immersion.

TABLE 9

SURFACE COMPOSITION (WT%) OF COPPER AFTER 3 DAYS OF IMMERSION IN 2M HNO_3 WITHOUT AND WITH THE OPTIMUM CONCENTRATIONS OF THE STUDIED INHIBITORS.

(Mass %)	Cu	C	O	N
Pure	100	--	--	--
Blank	72.63	--	21.33	6.04
Compound (1)	68.77	13.19	14.83	3.21
Compound (2)	67.14	12.17	15.26	5.43

3.8 Quantum Chemical Calculations

Figure (11) represents the molecular orbital plots and Mulliken charges of investigated compounds. Theoretical calculations were performed for only the neutral forms, in order to give further insight into the experimental results. Values of quantum chemical indices such as energies of lowest unoccupied molecular orbitals (LUMO) and energy of highest occupied molecular orbitals (HOMO) (E_{HOMO} and E_{LUMO}), the formation heat ΔH_f and energy gap ΔE , are calculated by semi-empirical AM1, MNDO and PM3 methods has been given in Table (10). It has been reported that the higher or less negative E_{HOMO} is associated of inhibitor, the greater the trend of offering electrons to unoccupied d orbital of the metal, and the higher the corrosion inhibition efficiency, in addition, the lower E_{LUMO} , the easier the acceptance of electrons from metal surface [54]. From Table (10), it is clear that ΔE obtained by the two methods in case of compound (2) is lower than compound (1), which enhance the assumption that compound (1) molecule will absorb more strongly on copper surface than compound (2), due to facilitating of electron transfer between molecular orbital HOMO and LUMO which takes place during its

adsorption on the metal surface and thereafter presents the maximum of inhibition efficiency. Also it can be seen that E_{HOMO} increases from compound (1) to compound (2) facilitates the adsorption and the inhibition by supporting the transport process through the adsorbed layer. Reportedly, excellent corrosion inhibitors are usually those organic compounds who are not only offer electrons to unoccupied orbital of the metal, but also accept free electrons from the metal [55,56]. It can be seen that all calculated quantum chemical parameters validate these experimental results.

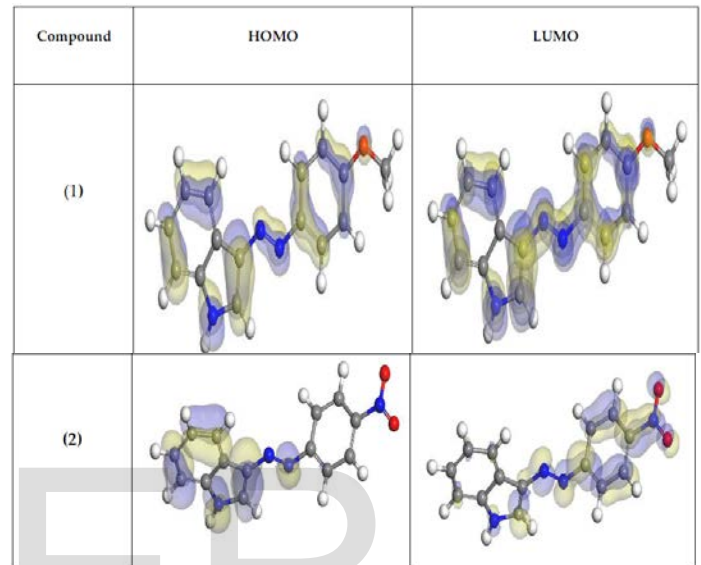


Fig. 11: Molecular Orbital Plots and Mulliken Charges of Organic Compounds

TABLE 10

THE CALCULATED QUANTUM CHEMICAL PROPERTIES FOR ORGANIC COMPOUNDS.

	Compound (1)	Compound (2)
$-E_{\text{HOMO}}$ (eV)	8.279	8.790
$-E_{\text{LUMO}}$ (eV)	1.126	0.581
ΔE (eV)	7.153	8.209
η (eV)	3.577	4.105
σ (eV-1)	0.280	0.244
$-\text{Pi}$ (eV)	4.703	4.686
χ (eV)	4.703	4.686
Dipole Moment (Debye)	2.768	8.680
Area (\AA^2)	282.137	280.471

3.9 Inhibition Mechanism

Inhibition of the corrosion of copper in 2M HNO_3 solution by investigated compounds is determined by

weight loss, potentiodynamic polarization measurements, electrochemical impedance spectroscopy (EIS), electrochemical frequency modulation method (EFM) and Scanning Electron Microscopy (SEM) studies, it was found that the inhibition efficiency depends on concentration, nature of metal, the mode of adsorption of the inhibitors and surface conditions.

The observed corrosion data in presence of these inhibitors, namely:

- i. The decrease of corrosion rate and corrosion current with increase in concentration of the inhibitor.
- ii. The linear variation of weight loss with time.
- iii. The shift in Tafel lines to higher potential regions.
- iv. The decrease in corrosion inhibition with increasing temperature indicates that desorption of the adsorbed inhibitor molecules takes place and the inhibition efficiency was shown to depend on the number of adsorption active centers in the molecule and their charge density.

The corrosion inhibition is due to adsorption of the inhibitors at the electrode/ solution interface, the extent of adsorption of an inhibitor depends on the nature of the metal, the mode of adsorption of the inhibitor and the surface conditions. Adsorption on copper surface is assumed to take place mainly through the active centers attached to the inhibitor and would depend on their charge density. Transfer of lone pairs of electrons on the nitrogen atoms to the copper surface to form a coordinate type of linkage is favored by the presence of a vacant orbital in copper atom of low energy. Polar character of substituents in the changing part of the inhibitor molecule seems to have a prominent effect on the electron charge density of the molecule.

It was concluded that the mode of adsorption depends on the affinity of the metal towards the π -electron clouds of the ring system. Metals such as Cu, which have a greater affinity towards aromatic moieties, were found to adsorb benzene rings in a flat orientation. The order of decreasing the percentage inhibition efficiency of the investigated inhibitors in the corrosive solution was as follow: compound (1) > compound (2).

Compound (1) exhibits excellent inhibition power due to: (i) the presence of p-OCH₃ group which is an electron donating group with negative Hammett constant ($\sigma = -0.27$). Also this group will increase the electron charge density on the molecule, (ii) its larger molecular size that may facilitate better surface coverage, and (iii) its adsorption through four active centers.

Compound (2) comes after compound (1) in inhibition efficiency. This is due to presence of p-NO₂ which has positive Hammett constant ($\sigma = +0.78$). i.e. group which lower the electron density on the molecule and hence, lower inhibition efficiency.

CONCLUSIONS

- All the investigated compounds are good corrosion inhibitors for copper in 2M HNO₃ solution. The effectiveness of these inhibitors depends on their structures. The variation in inhibitive efficiency depends on the type and the nature of the substituent present in the inhibitor molecule.

- EFM can be used as a rapid and nondestructive technique for corrosion measurements without prior knowledge of Tafel slopes.
- The results of EIS revealed that an increase in the charge transfer resistance and a decrease in double layer capacitances when the inhibitor is added and hence an increase in %IE. This is attributed to increase of the thickness of the electrical double layer
- Results obtained from potentiodynamic polarization indicated that the investigated derivatives are mixed-type inhibitors and a synergistic effect on %IE of a combination of the inhibitors and different anions were observed
- The adsorption of the inhibitors are adsorbed on copper surface obeys the Temkin adsorption isotherm model
- SEM-EDX images and analyses obtained in the presence of these compounds revealed the formation of thin film on the surface of copper
- The results obtained from chemical and electrochemical measurements were in good agreement. The order of %IE of these investigated compounds is in the following order: compound (1) > compound (2)
- The values of E_{HOMO} and E_{LUMO} decreases in an order runs parallel to the increase in %IE obtained which support the previous order

REFERENCES

- [1] H. Y. Tsai, S. C. Sun, S. J. Wang, J. Electrochem. Soc. 147 (2000) 2766.
- [2] A. Krishnamoorthy, K. Chanda, S. P. Murarka, G. Ramanath, J. G. Ryan, Appl. Phys. Lett. 78 (2001) 2467.
- [3] C. E. Ho, W. T. Chen, C. R. Kao, J. Electron. Mater. 30 (2001) 379.
- [4] R. R. Thomas, V. A. Brusica, B. M. Rush, J. Electrochem. Soc. 139 (1992) 678.
- [5] C. Fiaud, Proceedings of the Int. Symposium on Control of Copper and Copper Alloys Oxidation, Rouen, France, (1992) 97.
- [6] D. Chadwick, T. Hashemi, Corros. Sci. 18 (1978) 39.
- [7] S. L. F. A. da Costa, S. M. L. Agostinho, J. Electroanal. Chem. 296 (1990) 51.
- [8] H. A. A. El-Rahman, Corrosion 47 (1991) 424.
- [9] N. Bellakhal, K. Draou, A. Addou, J. L. Brisset, J. Appl. Electrochem. 30 (2000) 595.
- [10] M. M. El-naggar, J. Mater. Sci. 35 (2000) 6189.
- [11] F. Zucchi, G. Trabaneli, C. Monticelli, Corros. Sci. 38 (1996) 147.
- [12] D. Chadwick, T. Hashemi, Surf. Sci. 89 (1979) 649.
- [13] S. Yoshida, H. Ishida, Appl. Surf. Sci. 20 (1985) 497.
- [14] M. H. Wahdan, G. K. Gomma, Mater. Chem. Phys. 47 (1997) 176.
- [15] S. M. Song, C. E. Park, H. K. Yun, C. S. Hwang, S. Y. Oh, J. M. Park, J. Adhesion Sci. Technol. 12 (5) (1998) 541.
- [16] K. Hofmann, Imidazole and its Derivatives, Interscience Publishers, Inc, New York, 1953.
- [17] R. Ottana, R. Macari and R. Paola, J. Bio-org and Med Chem, 13 (2005) 4243.
- [18] R. W. Bosch, J. Hubrecht, W. F. Bogaerts, B. C. Syrett, Corrosion 57 (2001) 60.
- [19] S. S. Abdel-Rehim, K. F. Khaled, N. S. Abd-Elshafi, Electrochim. Acta .51 (2006) 6269.
- [20] A. N. Wiercinska, G. Dalmate, Electrochim. Acta. 51 (2006) 6179.
- [21] A. Yurt, A. Balaban, S. U Kandemir, G. Bereket, B. Erk, Mater Chem. Phys. 85(2004) 420.
- [22] A.Y. Etre, Appl. Surf. Sci. 252 (2006) 8521.
- [23] W. J. Lorenz and F. Mansfeld, Corros. Sci. 21 (1981) 647.
- [24] G. Trabaneli, in "Corrosion Mechanisms" (Ed. F. Mansfeld) Marcel Dekker, New York, 119 (1987).

- [25] A. S. Fouda, A. Abd. E. Aal, A. B. Kandil, J. Dasalination 201 (2006) 216.
- [26] F. H. Asaf, M. Abou- Krishna, M. Khodari, F. EL-Cheihk, A. A. Hussien, Mater Chem. Phys., 93 (2002) 1.
- [27] A. Fiala, A. Chibani, A. Darchen, A. Boulkamh, K. Djebbar, Appl. Surf. Sci. 253(2007) 9347.
- [28] S. T. Arab and E. M. Noor, Corrosion 49 (1993) 122.
- [29] W. Durnie, R. D. Marco, A. Jefferson, B. Kinsella, J. Electrochem. Soc., 146 (1999) 1751.
- [30] J. M. Thomas and W. J. Thomas, Introduction to the Principles of Heterogeneous Catalysis, 5th Ed, Academic Press, London (1981) 14.
- [31] G. Quartarone, G. Moretti, T. Bellomi, G. Capobianco, A. Zingales, Corrosion 54 (1998) 606.
- [32] W. D. Bjorndahl, K. Nobe, Corrosion 40 (1984) 82.
- [33] Schumacher, A. Muller, W. Stockel, J. Electroanal. Chem. 219 (1987) 311.
- [34] W. H. Smyrl, in: J. O. M. Bockris, B. E. Conway, E. Yeager, R. E. White (Eds.), Comprehensive Treatise of Electrochemistry, Plenum Press, New York. 4. (1981) 16.
- [35] G. Quartarone, T. Bellomi, A. Zingales, Corros. Sci. 45 (2003) 722.
- [36] J. W. Schlitz, K. Wippermann, Electrochim. Acta 32 (1987) 823.
- [37] D. C. Silverman and J. E. Carrico, National Association of Corrosion Engineers, 44 (1988) 280.
- [38] W. J. Lorenz and F. Mansfeld, Corros. Sci. 21 (1981) 647.
- [39] D. D. Macdonald, M. C. Mckubre. "Impedance measurements in Electrochemical systems," Modern Aspects of Electrochemistry, J. O'M. Bockris, B. E. Conway, R. E. White, Eds., Plenum Press, New York, New York, .14 (1962) 81.
- [40] F. Mansfeld; Corrosion, 36 (1981), 301.
- [41] C. Gabrielli, "Identification of Electrochemical processes by Frequency Response Analysis," Solarton Instrumentation Group, 1980.
- [42] M. El Achouri, S. Kertit, H. M. Gouytaya, B. Nciri, Y. Bensouda, L. Perez, M. R. Infante, K. Elkacemi, Prog. Org. Coat, 43 (2001) 267.
- [43] J. R. Macdonald, W. B. Johanson, in: J. R. Macdonald (Ed.), Theory in Impedance Spectroscopy, John Wiley & Sons, New York, 1987.
- [44] S. F. Mertens, C. Xhoffer, B. C. Decooman, E. Temmerman, Corrosion 53 (1997) 381.
- [45] G. Trabanelli, C. Montecelli, V. Grassi, A. Frignani, J. Cem. Concr., Res. 35 (2005) 1804.
- [46] A. J. Trowsdate, B. Noble, S. J. Haris, I.S. R. Gibbins, G. E. Thomson, G. C. Wood, Corros. Sci., 38 (1996) 177.
- [47] F. m. Reis, H. G. de Melo and I. Costa, J. Electrochem. Acta, 51 (2006) 17.
- [48] M. Lagrenee, B. Mernari, M. Bouanis, M. Traisnel & F. Bentiss, Corros. Sci., 44 (2002) 573.
- [49] E. Mc Cafferty, N. Hackerman, J. Electrochem. Soc. 119 (1972) 146.
- [50] H. Ma, S. Chen, L. Niu, S. Zhao, S. Li, D. Li, J. Appl. Electrochem 32 (2002) 65.
- [51] E. Kus, F. Mansfeld, Corros. Sci. 48 (2006) 965.
- [52] G. A. Caignan, S. K. Metcalf, E. M. Holt, J. Chem. Cryst. 30 (2000) 415.
- [53] M. Vajpeyi, S. Gupta, Dhirendra and G. N. Pandey, Corros. Prev. Control, October (1985) 102.
- [54] Samie, F., Tidblad, J., Kucera, V., Leygraf, C., 39, (2005) 7362.
- [55] amie, F., Tidblad, J., Kucera, V., Leygraf, C., 40, (2006) 3631.
- [56] I. Lukovits, K. Palfi, E. Kalman, Corrosion, 53 (1997) 915. 74- P. Zhao, Q. Liang, Y. Li, Appl. Surf. Sci., 252 (2005) 1596.